RSC Advances

Hydrodynamic on-rail droplet pass filter for fully passive sorting of droplet-phase samples

Journal:	*RSC Advances*
Manuscript ID:	RA-ART-08-2014-008354
Article Type:	Paper
Date Submitted by the Author:	08-Aug-2014
Complete List of Authors:	Yoon, Dong Hyun; Waseda University, Numakunai, Satoshi; Waseda university, Nakahara, Asahi; Waseda University, Sekiguchi, Tetsushi; Waseda University, Shoji, Shuichi; Waseda University, Department of Electronics, Information and Communication Engineering

Cite this: DOI: 10.1039/c0xx00000x

www.rsc.org/xxxxxx

PAPER

Hydrodynamic on-rail droplet pass filter for fully passive sorting of droplet-phase samples

Dong Hyun Yoon,*[a] Satoshi Numakunai,[a] Asahi Nakahara,[a] Tetsushi Sekiguchi,[b] and Shuichi Shoji[a]

Received (in XXX, XXX) Xth XXXXXXXXX 20XX, Accepted Xth XXXXXXXXX 20XX

DOI: 10.1039/b000000x

A hydrodynamic droplet pass filter for droplet-phase sample sorting was developed in this study. Using only groove rails, without additional components or external controls, droplets were sorted based on their physical properties. This is the first report of a droplet pass filter used for effective sorting, and the sorting structure provides a novel fluidic component for fluidic circuits for many applications. Depending on the number of rails, we obtained high-pass, low-pass, band-pass, and multi band-pass filters for sorting droplet samples, and their filtration performance was controlled by varying the dimensions of the rail structures. We evaluated in detail the effect of the rail width on sorting, threshold size of droplets sorted into each rail, and capillary number-dependent sample sorting. Furthermore, band-pass droplet sorting, useful for sample quantification, was provided, and multi-step rail ways allowed multi band-pass droplet sorting that was independent of flow conditions. The proposed sorting method does not require any external systems or skilled operation, and thus, it is expected that the device can contribute to on-site sample treatment and analysis in various fields such as medical care or the military.

Introduction

With the development of droplet-based chemistry and biochemistry, control and handling technologies for droplets have continuously progressed. Samples formed as microdroplets facilitate individualization,[1, 2] protection,[3, 4] and arrangement[5, 6] of the samples, as well as improved treatment efficiency. In particular, sample sorting is one of key pre- and post-treatment or analysis technologies. Well-sorted target samples ensure improved treatment and analysis results,[7] and sorting technologies have been developed according to the target's characteristics.

In many cases, droplet-phase samples are sorted by their optical properties. For instance, fluorescence-activated cell sorting utilizes the optical characteristics of the targets and they are sorted by applied electrical signals.[8, 9] In recent years, miniaturized platforms, using sophisticated systems to control samples more efficiently were also reported by many research groups. These are mainly based on electric-,[10–12] ultrasonic-,[13] hydrodynamic-,[14, 15] and optical-force-induces[16, 17] droplet driving, but the sorting performance fundamentally relies on detection or control elements. Therefore, the systems require complex components, not only for controlling actuators, but also for optical detection.

In contrast, magnetically labeled or electrically charged samples require a relatively simple sorting system. The systems are usually independent of the detection process, whether the samples are controlled actively or passively.[18, 19] However, the samples should have electro-magnetic characteristics, or should be labeled or charged for sorting. Consequently, sample types are limited and may also be exposed to undesirable chemicals or stimulations for the treatment and control.

Physical properties of samples, such as size, volume, density, viscosity, and surface tension are also important factors that affect droplet control and use. Because the amount of chemical or biological information is determined by the sample volume encapsulated within the droplet, the droplet size and volume are directly related to the analysis result.[20–22] Furthermore, the other properties are also closely related to the droplet's formation and behavior.[23–25] However, size or volume-dependent droplet sorting has been developed mostly using the active methods mentioned above, and passive sample sorting has been used in the case of particles and cells that are more solid than the droplet-phase samples.[26–29] Furthermore, viscosity-based passive droplet sorting has been recently reported,[30] but surface tension remains another important and interesting issue in various research fields.

In this research, we focused specifically on the droplet characteristics, and developed a novel method that can simultaneously and passively sort the droplets on the basis of their size and physical properties. The deformability of the droplet, which usually makes handling droplet-phase samples difficult, was utilized for sorting. Furthermore, Laplace pressure, crucial to droplet behavior, was also used for efficient sorting. In particular, parallel groove rails, reported by Baroud et al.,[31, 32] were implemented to obtain specific droplet behaviors. On the groove rails, the droplets were trapped, partially deformed, and conditionally sorted. Moreover, this is the first report that

discusses fully passive droplet sorting for different droplet sizes and physical properties without any additional systems or skilled operation.

Furthermore, this paper presents the development of fluidic components for use in various droplet filters. By varying the number and dimensions of the rails, we realized analogues for electronic high-pass, low-pass, band-pass, and multi band-pass filters in a fluidic circuit, and for the first time, their filtration performance was controlled.

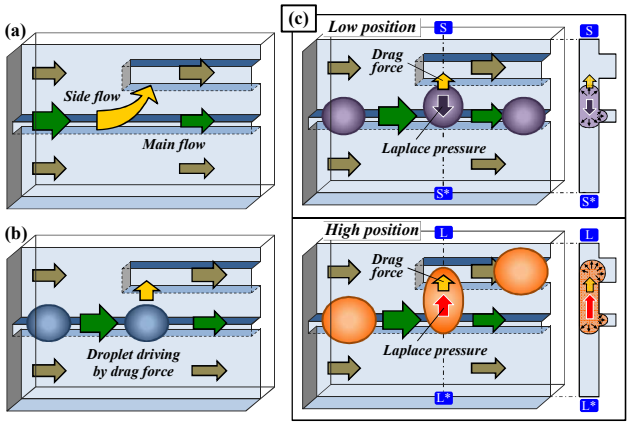

Fig. 1 Schematic view of a flow in a microchannel with parallel groove rails (a), hydrodynamic force on droplets introduced into the fluidic field (b), and deformation of the droplets by drag force and Laplace pressure (c).

Principle of passive droplet sorting

As shown in Figure 1(a), in a fluidic channel with a groove structure added on route, a main flow exists in the channel direction and a side flow exists in the groove direction. The flow in front of the new groove can be divided into flows along the tangential and normal directions, relative to the existing groove rail (hereafter referred to as the old rail). The tangential flow produces a driving force on droplets in the rail route, and the normal flow generates a drag force in the new groove. In contrast, as shown in Figure 1(b), droplets are trapped and follow the rail path due to the lower Laplace pressure on the rail in a Hele-Shaw cell with grooves.[31] However, when the droplets encounter the drag force due to the new rail, they are deformed and stretched, and the deformation amount varies with the physical properties of the droplets, e.g., radius and capillary number.[32]

As shown in Figure 1(c), when the droplet size or deformation is small, the droplet cannot reach the new rail, and the droplet recovers its shape and position because of the lower Laplace pressure in the old groove. In contrast, if the size or deformation of the droplet is large, a portion of the droplet will be located on the new rail, and the droplet would experience Laplace pressure in the new groove. Therefore, if the Laplace pressure in the new groove is lower than that in the old one, the droplet can transfer from the old rail to the new. Consequently, different membrane positions for the droplets on the rails allow condition-dependent droplet sorting, and that position is determined by the dimensions of the groove rails and the physical properties of the droplets.

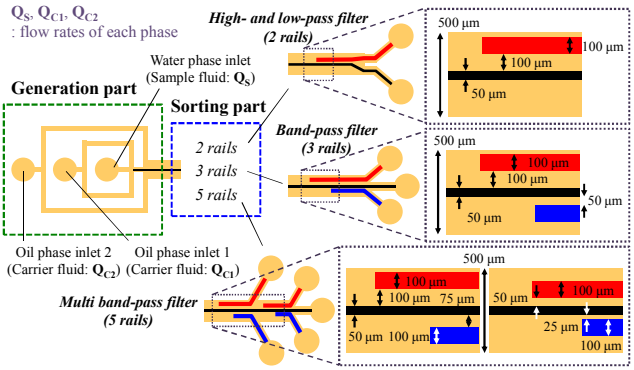

Fig. 2 Design of fluidic channel and detailed dimensions of rail patterns for each type of droplet sorting device.

Device design and fabrication

Design of the droplet-pass filters

The droplet sorting device consisted of a droplet generation part and a sorting part, as shown in Figure 2. Droplets were generated at the cross junction and they were sorted by the rails. One sample fluid and one carrier fluid were introduced for droplet generation, and one additional carrier flow was employed, for the control of the distance between the droplets and total flow rate. In addition, three types of groove rails–with two, three, and five rail ways–are discussed. In all cases, the heights of the channels and grooves were 50 μm.

As the first step for droplet sorting, the behavior of droplets on two groove rails was determined. In particular, the transfer of droplets on the basis of their size, and the variation in the droplet transfer depending on the rail types and droplet materials were examined. In the second step, the droplet transfer was expanded in both directions for an old rail, using two new rails with different distances. Finally, two-step sorting using five rail ways, was investigated for multiple sorting of various droplet sizes. Specifically, droplet sorting corresponding to a high-pass, low-pass, band-pass, or multi band-pass filter of an electric circuit was performed in a fluidic device using two, three, or five rails, respectively. Furthermore, droplet sorting under different volume flow rates was evaluated.

Device fabrication

The sorting device was fabricated using a soft lithography process using PDMS (polydimethylsiloxane) (SILPOT 184, Dow Corning) and SU-8 photo resist (Microchem). In particular, a two-layer SU-8 mold was formed for fluidic channels and groove rails. Using O2 plasma treatment (Aiplasma, Matsushita Electric Works), the PDMS structure was bonded onto a PDMS spin-coated glass substrate to obtain a structure fully surrounded by PDMS.

Experiments and discussion

Experimental setup and materials

Syringe pumps (KDS210, KD Scientific) were the only equipment associated with liquid injection, droplet generation, and sorting in this device and system. Salad oil was used as the carrier fluid, and the droplets were generated using a methylene blue aqueous solution for fine visualization. Furthermore, acetic

acid was used to obtain different physical properties. The droplet generation and sorting behavior were visualized by using a high-speed camera (FASTCAM-NEO, Photron), and the droplet size was calculated by pixel counting for the collected droplets in the outlet.

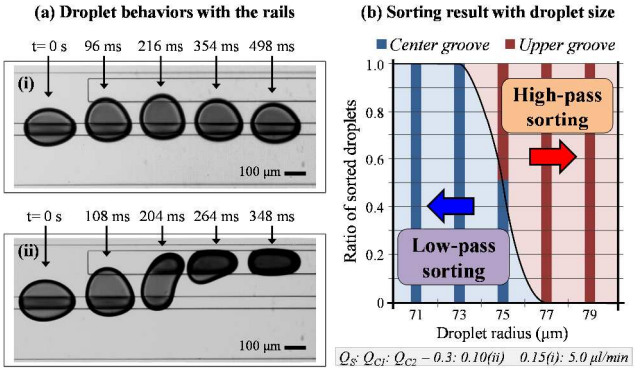

Fig. 3 Different droplet routes and deformation behaviors in the rail channel due to size, and size-dependent high or low-pass sorting of the droplets in the two rails.

High-pass and low-pass droplet sorting using two groove rails

Size-dependent droplet sorting between two rails was visualized, as shown in Figure 3(a) and ESI† Movie 1. Initially, droplets were introduced from the old rail, and then, the droplets were sorted into different rail ways according to their size. In both cases, the droplets were deformed by the new rail, but only a large droplet's size was sufficient to shift the droplet to a new rail. The behavior of the droplets that were not transferred show that the side flow to the new rail is limited to a short area. Outside of the drag area, small droplets recovered their shape due to Laplace pressure in the old rail. In contrast, the highly deformed large droplets faced lower Laplace pressure in the new rail; therefore, the droplets can transfer to the new rail. All droplets with radii larger than 77 μm were shifted to the new rail, and droplets with radii smaller than 73 μm remained entirely on the old rail, as shown in Figure 3(b).

Droplet sorting analogous to the high or low-pass filter of an electric circuit was evaluated by varying the rail width, distance between rails, and physical properties. Firstly, new rails with the same and smaller width were used to determine the effect of the rail width on the droplet transfer, as shown in Figure 4(a). In the case of the same rail width, the droplets located on both rails were not deformed or shifted to one side, because the Laplace pressure of the droplets on the grooves is equivalent. In contrast, when the narrow rail was used, the centers of droplets were closer to the old rail. These results indicate that for droplet transfer, the width of the new rail should be larger than that of the old rail.

Secondly, two distances between the old and new rail, 50 μm and 100 μm, were compared to investigate the effect of rail separation on sorting. As shown in Figure 4(b), because the new rail at 100 μm separations required larger deformation of droplets, the threshold radius of droplets sorted into the new rail at a distance of 100 μm was larger than that for the 50 μm distance. These results show that the distance between rails can be used as a parameter to control the sorting performance.

Finally, the droplet physical properties that may influence sorting were considered. Deionized water and a 5% acetic acid aqueous solution were used for verification of this influence. In particular, because the acetic acid has a high viscosity and low surface tension, the capillary number of the solution is larger than that of pure water. Therefore, the high capillary number led to substantial deformation of droplets in the direction of the new rail. This result produced a different threshold radius for droplets sorted into the new rail; the droplets formed by the acetic acid-dissolved solution that were shifted to the rail had smaller radii than water droplets, as shown in Figure 4(c). This indicates that the rail structure is capable of capillary number-dependent as well as size-dependent droplet sorting.

Band-pass droplet sorting using three groove rails

The parallel rail ways were expanded for multiple size droplet sorting. New rails were located in sequence on both sides of an old rail, and the distances to the first and second new rails from the old rail were 100 μm and 50 μm, respectively. Therefore, the three rails could sort different-sized droplets, and the results are shown in Figure 5 and ESI† Movie 2. All droplets with radii larger than 85 μm were sorted into the upper rail and droplets with radii less than 65 μm were almost completely sorted into the center rail. In particular, droplets sorted by the lower rail form a range of droplet sizes. The band pass sorting can be applied to the quantification of droplet-phase samples. The band-width of the droplet radius was approximately 10 μm broadly, because only two rail distances were present in this step. However, it is expected that a smaller rail separation would allow narrower band-width for the sorted droplet sizes.

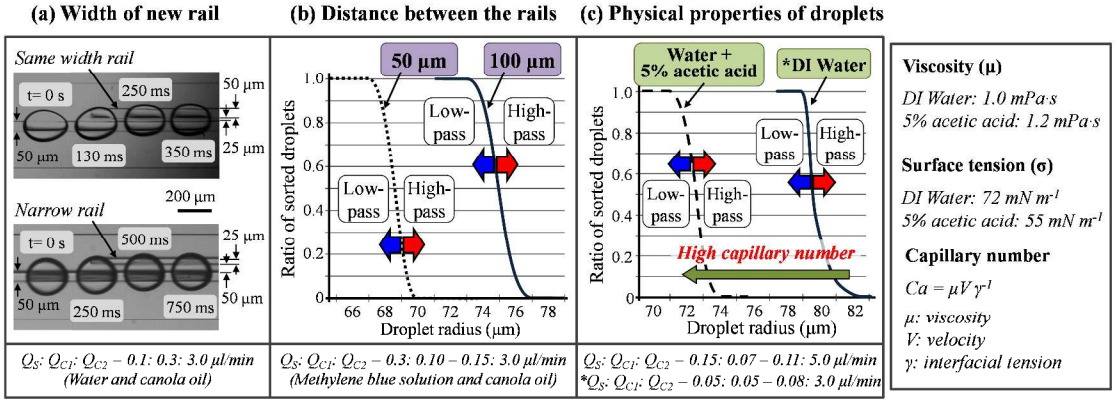

Fig. 4 Effects of width of the new rail (a), distance between old and new rail (b), and physical properties of droplets (c) on droplet sorting results.

Cite this: DOI: 10.1039/c0xx00000x

www.rsc.org/xxxxxx

PAPER

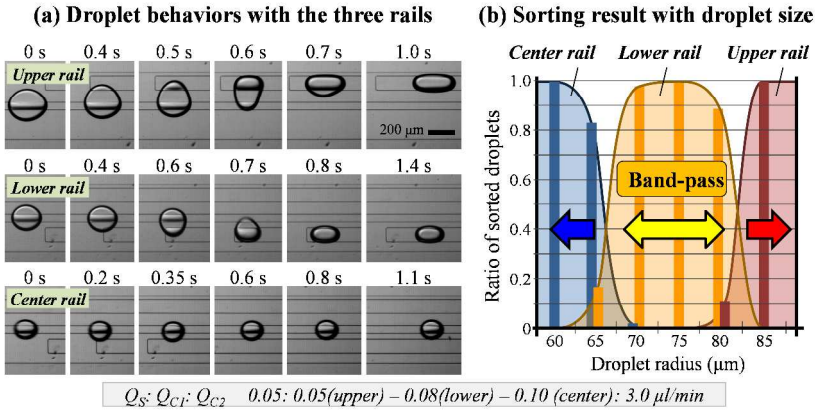

Fig. 5 Band-pass droplet sorting using three rails: visualization of droplet transfer on the rail ways (a) and the range of droplet sizes sorted into each rail (b).

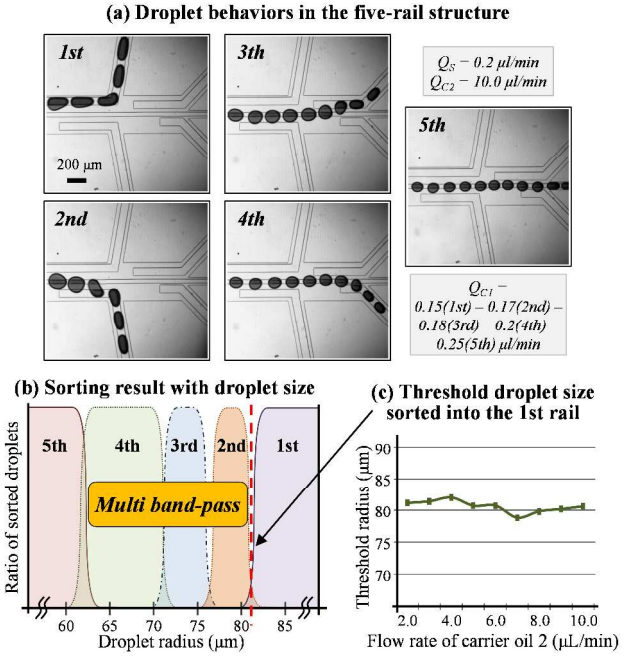

Fig. 6 Multi band-pass droplet sorting via five rails: visualized route of droplets into each rail (a), the band pass of the sorted droplets (b), and evaluation of the effect of flow speed on the droplet sorting (c).

Multi band-pass droplet sorting using five groove rails

Finally, multi-step sorting was examined using four rails with an old rail. Rails with large separations, 100 μm and 75 μm, for relatively large sized droplet sorting were implemented as the first step, and rails with smaller separations, 50 μm and 25 μm, were inserted for the second step of sorting. Droplets of different sizes, initially introduced from the old rail, were sorted into different rail ways according to their size, as shown in Figures 6(a), 6(b), and ESI† Movie 3. As a result, the size of the sorted droplets formed multiple bands. The maximum radius of droplets on the old rail was 62 μm, and minimum radius of droplets sorted into the first rail was 82 μm. Furthermore, the band-widths of the radii of the droplets sorted by the fourth, third, and second rails were approximately 10, 5, and 5 μm, respectively. In particular, the width of the fifth outlet was narrower than that of the other outlets, to prevent droplets from merging into each other due to a decrease in the flow rate. Therefore, it appears that the band width of the fourth rail was relatively large, due to an increase in the flow resistance in the fifth channel. However, overall volume-dependent droplet sorting was successfully performed via the different separations of the groove rails.

Figure 6(c) shows the threshold radius of droplets sorted into the first new rail via different total flow rates. Even though the flow rates varied, the sorted droplet size was almost independent of the flow. This result is because, at the front of the new rail, the ratio of flow rates in the direction of the old and new rails is uniform, and the flow into the new rail exists in a limited area only. Under this condition, the drag force for the new rail increases with the large flow rate, but the drag force for the old rail also increases with the flow. Therefore, the time for droplet deformation in the new rail decreases in a limited area, and the positions of the droplets were uniform under different flow conditions. This flow-independent result would ensure stable sorting performance for various systems utilizing the proposed method.

Conclusions

The microfluidic devices utilizing parallel groove rails successfully achieved size-dependent high-pass, low-pass, band-pass, and multiple band-pass droplet sorting. The droplets on an existing groove rail were transferred to new rails by the drag force resulting from the side flow into the new rails. The sorting performance was controlled by changing the dimensions of the groove structure, in particular, the width of the new rail and distance between the rails. Moreover, the droplets could be sorted according to the capillary number of the sample fluids. In contrast, the number of the rails determined the type of the sorting. Three rails with different separation provided band-pass

sorting of the droplets according to size. Furthermore, the number of bands was simply increase by increasing the number of rails, and the band-width could be improved by varying the rail separation.

This droplet sorting was carried out completely without any additional external control. Therefore, the droplets are free from any damage caused by active control, such as those caused by electric signals, magnetic fields, or mechanical operations. Furthermore, the droplet sorting had little dependence on the total flow rate. Hence, the droplet sorting scheme is suitable for quantification of sample volumes for chemical or biological treatment and analysis, and may be a useful complement to devices that significantly disturb the fluid flow.

Acknowledgment

This work is partly supported by the Japan Ministry of Education, Culture, Sports Science & Technology (MEXT) Grant-in-Aid for Scientific Basic Research (S) No. 23226010.

Notes and references

[a] *Faculty of Science and Engineering, Waseda University, 3-4-1, Okubo, Shinjuku, Tokyo, Japan. Tel: +81 3 5286 3384; E-mail: yoon@shoji.comm.waseda.ac.jp*
[b] *Institute for Nanoscience and Nanoengineering, Waseda University, 513, Tsurumaki-cho, Waseda, Shinjuku, Tokyo, Japan*

† Electronic Supplementary Information (ESI) available: droplet sorting behaviors using the different rail ways. See DOI: 10.1039/b000000x/
‡ Footnotes should appear here. These might include comments relevant to but not central to the matter under discussion, limited experimental and spectral data, and crystallographic data.

1 M. Chabert and J. L. Viovy, *Proc. Natl. Acad. Sci.*, 2008, **105**, 3191.
2 W. Shi, J. Qin, N. Ye, and B. Lin, *Lab Chip*, 2008, **8**, 1432.
3 T. Douglas and M. Young, *Nature*, 1998, **393**, 152.
4 T. Wang, I. Lacik, M. Brissova, A. V. Anilkumar, A. Prokop, D. Hunkeler, R. Green, K. Shahrokhi, and A. C. Powers, *Nat. Biotechnol.*, 1997, **15**, 358.
5. G. S Du, J. Z. Pan, S. P. Zhao, Y. Zhu, J. M. J. den Toonder, and Q. Fang, *Anal. Chem.*, 2013, **85**, 6740.
6. A. C. Hatch, J. S. Fisher, A. R. Tovar, A. T. Hsieh, R. Lin, S. L. Pentoney, D. L. Yang, and A. P. Lee, *Lab Chip*, 2011, **11**, 3838.
7. L. Mazutis, J. Gilbert, W. L. Ung, D. A. Weitz, A. D. Griffiths, and J. A. Heyman, *Nature protocols*, **8**, 870.
8. Fulwyler MJ (1965) Electronic separation of biological cells by volume. Science 150: 910–911.
9. M. T. Anderson, I. M. Tjioe, M. C. Lorincz, D. R. Parks, L. A. Herzenberg, G. P. Nolan, and L. A. Herzenberg, *Proc. Natl. Acad. Sci. USA*, 1996, **93**, 8508.
10. B. E. Debs, R. Utharala, I. V. Balyasnikova, A. D. Griffiths, and C. A. Merten, *Proc Natl Acad Sci.*, 2012, **109**, 11570.
11. J. C. Baret, O. J. Miller, V. Taly, M. Ryckelynck,a A. El-Harrak, L. Frenz, C. Rick, M. L. Samuels, J. B. Hutchison, J. J. Agresti, D. R. Link, D. A. Weitz, and A. D. Griffiths, *Lab chip*, 2009, **9**, 1850.
12. D. R. Link, E. Grasland-Mongrain, A. Duri, F. Sarrazin, Z. Cheng, G. Cristobal, M. Marquez, and D. A.Weitz, *Angew. Chem. Int. Ed.*, 2006, **45**, 2556.
13. C. Lee, J. Lee, H. H. Kim, S. Y. Teh, A. Lee, I. Y. Chung, J. Y. Park, and K. K. Shung, *Lab chip*, 2012, **12**, 2736.
14. Z. Cao, F. Chen, N. Bao, H. He, P. Xu, S. Jana, S. Jung, H. Lian, and C. Lu, *Lab chip*, 2013, **13**, 171.
15. H. Maenaka, M. Yamada, M. Yasuda, and M. Seki, *Langmuir*, 2008, **24**, 4405.
16. C. N. Baroud, J. P. Delville, F. Gallaire, and R. Wunenburger, *Phys. Rev. E*, 2007, **75**, 046302.
17. E. Fradet, C. McDougall, P. Abbyad, R. Dangla, D. McGloin, and C. N. Baroud, *Lab Chip*, 2011, **11**, 4228.
18. Y. Wang, Y. Zhao, and S. K. Cho, *J. Micromech. Microeng.*, 2007, **17**,2148.
19. A. Chen, T. Byvank, W. J. Chang, A. Bharde, G. Vieira, B. L. Miller, J. J. Chalmers, R. Bashird, and R. Sooryakumar, *Lab Chip*, 2013, **13**, 1172.
20. J. W. Choi, D. K. Kang, H. Park, A. J. deMello, and S. I. Chang, *Anal. Chem.*, 2004, **84**, 3849.
21. K. Leung, H. Zahn, T. Leaver, K. M. Konwar, N. W. Hanson, A. P. Page, C. C. Lo, P. S. Chain, S. J. Hallam, and C. L. Hansen, *Proc. Natl. Acad. Sci*., 2012, **109**, 7665.
22. A. R. Abate, T. Hung, R. A. Sperling, P. Mary, A. Rotem, J. J. Agresti, M. A. Weinere, and D. A. Weitz, *Lab Chip*, 2013, **13**, 4864.
23. T. D. Tice, A. D. Lyon, and R. F. Ismagilov, *Analytica Chimica Acta*, 2004, **507**, 73.
24. M. G. Simon, R. Lin, J. S. Fisher, and A. P. Lee, *Biomicrofluidics*, 2012, **6**, 014110.
25. A. Vananroye, P. V. Puyvelde, and P. Moldenaers, *Langmuir*, 2006, **22**, 3972.
26. M. Yamada and M. Seki, *Lap Chip*, 2005, **5**, 1233.
27. D. W. Inglis, *Appl. Phys. Lett.*, 2009, **94**, 013510.
28. H. M. Ji, V. Samper, Y. Chen, C. K. Heng, T. M. Lim, L. Yobas, *Biomed. Microdevices*, 2008, **10**, 251.
29. S. S. Shevkoplyas, T. Yoshida, L. L. Munn, and M. W. Bitensky, *Anal. Chem.*, 2005, **77**, 933.
30. A. C. Hatch, A. Patel. N. R. Beer, and A. P. Lee, *Lab Chip*, 2013, **13**, 1308.
31. P. Abbyad, R. Dangla, A. Alexandrou, and C. N. Baroud, *Lab Chip*, 2011, **11**, 813.
32. R. Dangla. S. Lee, C. N. Baroud, *Phys. Rev. Lett.*, 2011, **107**, 124501.